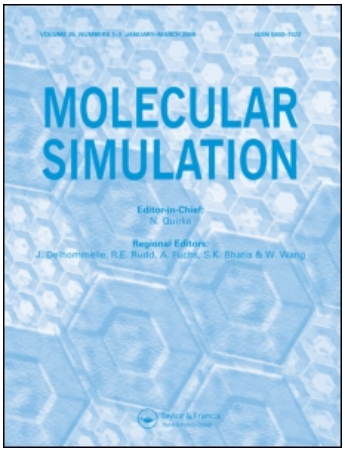

Molecular Simulation

Publication details, including instructions for authors and subscription information:
http://www.informaworld.com/smpp/title~content=t713644482

Bonding and Stability of Hybrid Diamond/Nanotube Structures

O. A. Shenderova[a]; D. Areshkin[a]; D. W. Brenner[a]
[a] Department of Materials Science and Engineering, North Carolina State University, Raleigh, NC, USA

Online publication date: 26 October 2010

To cite this Article Shenderova, O. A. , Areshkin, D. and Brenner, D. W.(2003) 'Bonding and Stability of Hybrid Diamond/Nanotube Structures', Molecular Simulation, 29: 4, 259 — 268
To link to this Article: DOI: 10.1080/0892702021000049691
URL: http://dx.doi.org/10.1080/0892702021000049691

Molecular Simulation, 2003 Vol. 29 (4), pp. 259–268

Bonding and Stability of Hybrid Diamond/Nanotube Structures

O.A. SHENDEROVA*, D. ARESHKIN and D.W. BRENNER

Department of Materials Science and Engineering, North Carolina State University, Raleigh, NC 27695-7907, USA

(Received May 2002; In final form September 2002)

Geometrical considerations combined with detailed atomic modeling are used to define general classes of diamond/carbon nanotube interface structures with low residual stresses and no unsatisfied bonding. Chemically and mechanically robust interfaces are predicted, supporting recent experimental studies in which structures of this type were proposed.

Keywords: Hybrid structures; Diamond; Nanotube; Bonding and stability

INTRODUCTION

Several recent experiments have provided compelling evidence for stable hybrid carbon nanotube-diamond structures. In experiments by Kuznetsov *et al.* [1,2] the formation of nanometric closed curved graphitic structures with tubular or conical forms attached to a surface of a diamond particle were observed in high-resolution transmission electron microscopy (TEM) images of diamond particles after high-temperature annealing. The TEM images show concentric graphitic shells corresponding to the top view of nested carbon nanotubes as well as a side view of nanotubes on the edges of particles. The authors suggest that multi-layered graphitic caps that form during the initial annealing of micron-sized diamond particles at 1800–2000 K transform into closed carbon nanotubes attached to the diamond surface via reconstruction of the edges of diamond (111) planes orthogonal to the surface into graphite (0001) planes. Avigal *et al.* [3] and Ayres *et al.* [4] have also recently reported simultaneous growth of hybrid structures of diamond crystallite and carbon nanotubes on the same substrate by plasma-enhanced chemical vapor deposition.

There is an interesting and widely recognized geometrical similarity between the {111} planes of diamond and individual graphene sheets in which pairs of diamond planes resemble "puckered" graphite. This geometrical relationship together with the lengthening of carbon–carbon bonds from 1.42 Å in graphite to 1.54 Å in diamond results in the near epitaxial relations [14]

$$\text{Graphite}\,(0001)\|\text{diamond}\,(111)$$

$$\text{Graphite}\,[11\bar{2}0]\|\text{diamond}\,[10\bar{1}]$$

between graphite and diamond planes (Fig. 1). Several graphite–diamond interface structures have been modeled based on these general relations. Lambrecht *et al.* for example, used an analytic potential to characterize graphite planes bonded to diamond as a model for diamond nucleation on graphite [5]. Shenderova and Brenner have explored similar structures as graphitic occlusions in diamond grain boundaries [6]. Balaban *et al.* have characterized the electronic properties of structures in which graphitic sections of varying widths are connected by rows of sp^3-bonded carbon [7]. Transitions between diamond and graphitic structures have also been explored as models for the graphitization of diamond surfaces and clusters [8,9].

In work related to that presented here, several specific closely matched diamond-fullerene nanotube interface structures have been modeled. Sinnott and coworkers, for example, used atomic simulations to model bonded interfaces between diamond {111} surface planes and (6, 0) fullerene nanotubules [10]. For a sufficiently high density of bonded

*Corresponding author. Fax: +1-919-515-7724. E-mail: oashend@eos.ncsu.edu

ISSN 0892-7022 print/ISSN 1029-0435 online
DOI: 10.1080/0892702021000049691

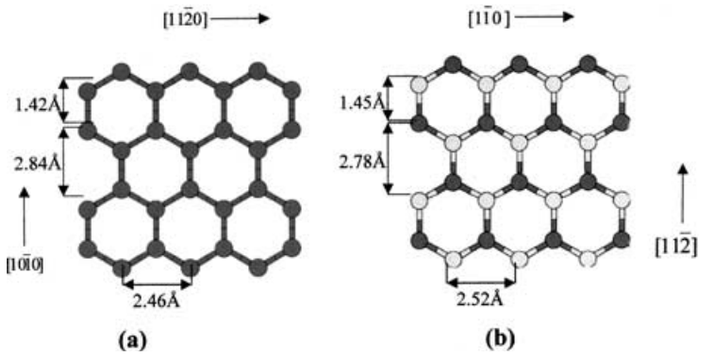

FIGURE 1 Illustration of a (a) graphene and (b) diamond (111) plane viewed along the ⟨111⟩ projection. The lighter shadowed circles in the diamond structure represent raised atoms. Distances between diamond atomic sites are measured in the (111) plane.

nanotubes, these structures are predicted to have elastic moduli comparable to diamond but at a lower overall density. Shenderova *et al.* have also modeled nanotube/nanodiamond cluster combinations consisting of (12, 0) and (6, 0) nanotubes bonded to cubo-octahedron diamond particles, and a (5, 5) nanotube bonded to a penta-particle [11].

Motivated by the recent experiments discussed above, we have modeled a broad range of nanotube-diamond hybrid structures, from which generalized rules for forming stable structures of this type have been developed. These results, which are reported below, suggest that a variety of mechanically and chemically stable diamond/nanotube structures without dangling bonds at the interface are possible. These structures include both metallic and semiconducting nanotubes bonded to diamond clusters or substrates. Hence, different types of heterojunctions are theoretically feasible for carbon-based nanoelectronics applications, including diodes, novel quantum dots, and robust field emitters [12].

SIMULATION TECHNIQUES

Identifying potentially stable bonding interface structures requires determining sites available for bonding at an edge of an open nanotube and those on a free diamond surface such that the maximum number of bonds between the two structural components are formed. To initially define general geometrical trends that fulfill this requirement between different types of carbon nanotubes and (111) and (001) diamond surfaces, a grid corresponding to atomic sites on a particular diamond surface and a polygon with vertexes corresponding to radical sites at an edge of a specific tube were generated (Fig. 2). By rotating and translating the polygons along the grid, positions c were determined such that the maximum number of polygon vertices are near grid points (Fig. 2). In cases where multiple possible structures were determined, lateral mismatches between individual grid points and polygon vertices were used to efficiently choose the most likely lowest-energy structure. After being generated, all of the structures reported below were relaxed to their minimum energy configurations using an analytic many-body bond-order potential energy function for hydrocarbons [13]. Atomic level residual stresses and interface energies of the hybrid structures were then calculated using the same analytic potential. The interface energy was calculated as the difference between the energy of the atoms at the interface and the energy per atom in the ideal systems. The reference point for atoms at the diamond side of an interface is the energy per atom in ideal diamond (-7.37 eV) calculated with the bond order potential, while for example

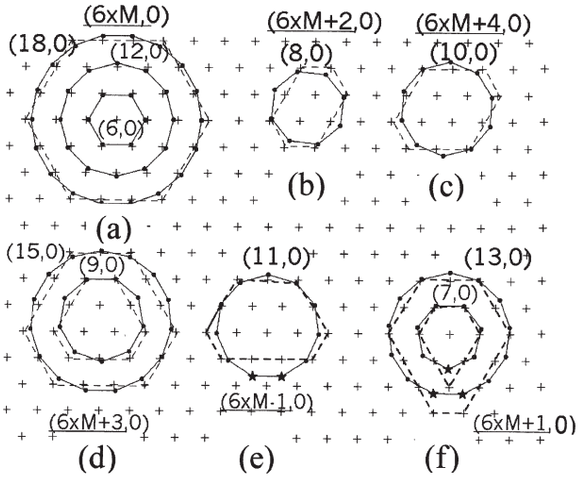

FIGURE 2 Schemes for the possible connection between a (111) diamond surface and zigzag nanotubes. Dots connected by solid lines correspond to the atomic sites available for bonding at nanotube edges. Crosses correspond to atomic sites at the (111) diamond surface. Dashed lines connect sites on the diamond surface participating in the bonding with the specific nanotube. Stars at the contours of the (11, 0) and (13, 0) nanotubes denote the dangling bonds at the diamond/nanotube interface after nanotube attachment.

the reference point for atoms in a graphene structure is the energy per atom in ideal graphene (-7.39 eV). When instead of graphene a hybrid structure containing a nanotube is examined, the reference point for the nanotube was chosen as the energy per atom of the corresponding relaxed infinite nanotube. The total surface area of the interface was calculated as the area per atom on the diamond surface multiplied by the number of bonds per interface. This facilitates comparisons between grain boundary energies, for example, and the interface energies calculated here.

The analytic potential energy function [13] is a many-body bond order potential that mimics bonding in carbon systems for a wide range of atomic hybridizations. The function reproduces a relatively large database of molecular properties of hydrocarbons as well as solid-state properties of carbon, including the in-plane lattice constant, cohesive energy and elastic properties of graphene sheets as well as the cohesive energy and elastic properties of diamond.

DIAMOND/NANOTUBE STRUCTURES: GEOMETRICAL COMPATIBILITY

The analysis presented here is restricted to nanotubes perpendicularly attached to diamond (001) and (111) facets. This restriction requires that the plane of an edge of an open nanotube be perpendicular to the tube axis. Only $(n, 0)$, or zigzag, and (n, n), or armchair types of nanotubes were considered because all dangling bonds of the nanotube edges are within the same plane, and the bond density is high compared to chiral nanotubes. The high bond density presumably results in strong bonding for zigzag and armchair nanotubes as compared to chiral structures.

Bonding Between Graphene and Diamond

For completeness, a brief analysis of bonding between a diamond surface and the edge of a graphene sheet is presented. The $(10\bar{1}0)$ and $(11\bar{2}0)$ edges of graphene (Fig. 1) correspond to the ends of zigzag and armchair nanotubes, respectively; therefore only these edges are considered. For each graphene edge, it is necessary to define a corresponding line of carbon atoms within a diamond crystal such that the pattern of distribution of atomic sites along the line will be as close as possible to the pattern of distribution of dangling bonds along the graphene edge. Only a 2.4% lattice mismatch exists between any diamond plane containing a $\langle 110 \rangle$ vector and a zigzag edge of a graphene sheet. All low-index diamond surfaces ((100), (110) and (111)) contain a $\langle 110 \rangle$ vector and, therefore, can be attached to graphene along its zigzag edge. The bonding strength, however, depends on the local environment of the diamond surface atoms, which are specific for particular diamond surfaces. For example, atoms at the (111) diamond surface are three-fold coordinated (Fig. 3a), while those at the (100) surface are two-fold coordinated (Fig. 3b). Thus, atoms at the (100) surface will not be fully coordinated after attachment of a graphene sheet and the interface energy will be higher than that for the (111) diamond surface. Due to the structural anisotropy along the $\langle 011 \rangle$ and $\langle 0\bar{1}1 \rangle$ directions on the (100) diamond surface, there also exists a difference in the interface energy between graphene attached along these two directions (Table I).

One possibility for decreasing the interface energy between the (100) diamond surface and graphene is the reconstruction of the (100) surface resulting in three-fold coordination of the surface atoms, such as, for example, dimer formation along the $\langle 0\bar{1}1 \rangle$ direction (Fig. 3c). However, attachment of graphene to the dimerized (100) diamond surface is not predicted to result in energy gain, as might be expected from the resulting four-fold coordination of the surface sites (Table I). This is because the energies of the subsurface atoms are high due to distortions caused by dimerization and the overall interface energy for the reconstructed surface is predicted to be higher than that of the unreconstructed surface (Table I). Interface bond lengths between a zigzag graphene edge and (111) and (100) diamond surfaces are also given in Table I. Graphite planes attached to the {112} diamond surface along the $\langle 0\bar{1}1 \rangle$ direction have been previously characterized by Lambrecht *et al.* [5] At this relative orientation of diamond and graphite, graphite planes are spatially extended to the (111) diamond planes inside a diamond crystal.

Finding low-stress structures connecting an armchair edge of graphene to diamond is more difficult then for the graphene zigzag edge. Because of a very high lattice mismatch (43%) between unreconstructed diamond (111) and (100) surfaces and the armchair edge of graphene, it is not possible to obtain uniform bonding along the interface with all bonds saturated. A reconstructed (111) diamond surface, (e.g. Pandey chain formation) as well as the reconstructed (100) 2×1 surface also posses high lattice mismatch (more than 20%) with the armchair edge of graphene. This resulted in the appearance of the interface dislocations within the graphene plane during atomistic simulations (Fig. 3d).

Although it is impossible to connect atom-to-atom an armchair edge of graphite and the (111) and (100) diamond surfaces, there are some possibilities for other surfaces. Very low mismatch (2%) exists between an armchair edge of graphene and atomic sites along the $\langle 1\bar{2}1 \rangle$ direction of the (111) diamond plane projected along the $\langle 111 \rangle$ direction (Fig. 1).

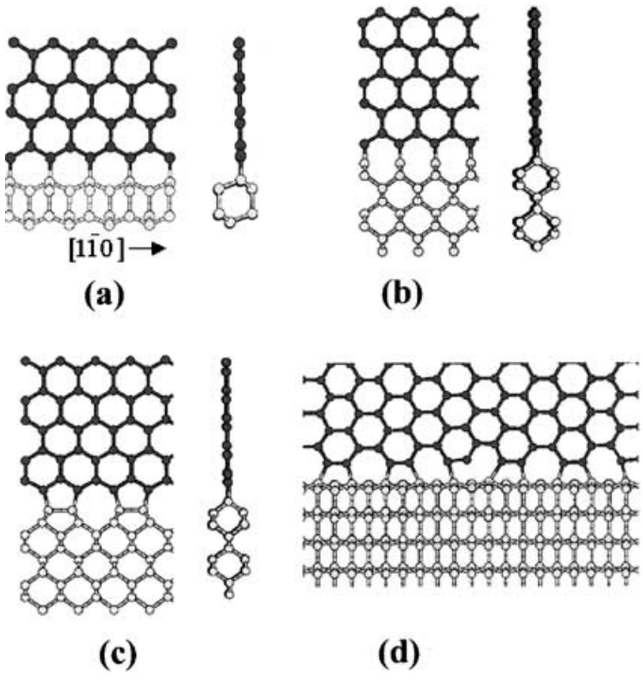

FIGURE 3 Illustration of various graphene–diamond interface structures. (a) A zigzag edge of graphene and the (111) diamond surface. (b) A zigzag edge of graphene and an unreconstructed (100) diamond surface, along the ⟨0$\bar{1}$1⟩ direction. (c) A zigzag edge of graphene and the reconstructed (100) diamond surface, along the ⟨0$\bar{1}$1⟩ direction. (d) Structure of the interface between an armchair edge of graphene and the reconstructed (100) 2 × 1 surface. Dark spheres correspond to graphene atoms, light spheres correspond to diamond atoms. Front and side views of the interfaces (a)–(c) are shown.

However in three-dimensional space the distances between sites available for bonding are 1.54 and 2.95 Å, and a slight corrugation of a graphene edge near the interface takes place (Fig. 4a). In this case graphene can be attached to the (110) diamond plane along two adjacent rows of ⟨1$\bar{2}$1⟩-oriented atomic sites (Fig. 4a). An armchair edge of graphene can also be attached to the {112} and {110} planes in the londsdalite structure along two adjacent rows oriented along the ⟨111⟩ direction with inter-site distances 1.54 and 2.57 Å (Fig. 4b). Graphene can be also attached to the {110} londsdalite plane along two adjacent rows of ⟨1$\bar{2}$1⟩-oriented atomic sites with inter-site distances 1.54 and 2.95 Å (Fig. 4b). A slight corrugation of a graphene edge near the interface would take place in this case. The possibility of attachment of the armchair edge of graphene to the (110) londsdalite plane also suggests that graphene can be, in principle, attached to the (110) diamond surface containing stacking faults along the lines of intersection of a stacking fault with the (110) diamond surface.

Bonding Between Nanotubes and (111) Diamond Facet

As reported above, among possible hybrid structures between graphene and diamond, the lowest interface energy was calculated for graphene attached along its zigzag edge to the (111) diamond surface (Table I). The same is true for zigzag nanotubes, a wide variety of which can be attached to the (111) diamond

TABLE I Energetic and bond length parameters for the interface between diamond surfaces and the zigzag edge of graphene calculate using the bond-order potential [13]

		Energy per atom (eV)		
Diamond surface	*Interface energy (J/m^2)*	*Diamond*	*Graphene*	*Interface bond length (Å)*
(111)	0.41	−7.5	−7.12	1.52
(100), ⟨011⟩	2.74	−6.30	−7.40	1.425
(100), ⟨0$\bar{1}$1⟩	1.86	−6.5	−7.52	1.40
(100) − 2×1, ⟨0$\bar{1}$1⟩	2.90	−7.04 (6.92*)	−7.02 (1.7 for dimer)	1.52

* Energy per atom for a first diamond neighbor of a dimerized diamond atom at the interface.

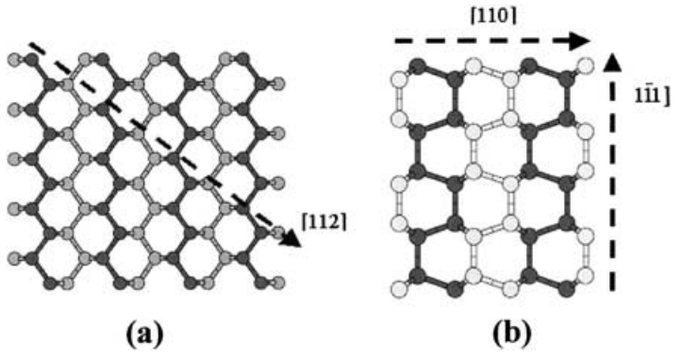

FIGURE 4 Illustration of the (110) planes in (a) diamond and (b) londsdalite structures. Dashed lines correspond to rows of atomic sites along which graphene can be attached along its armchair edge to raised atoms at the surfaces, indicated by lighter circles. There can be a single row of atoms (e.g. structure (b), ⟨111⟩ direction) or two adjacent rows of atoms (e.g. structures (a) and (b) ⟨112⟩ direction).

surface. After "wrapping" up a piece of graphene to form a nanotube, the distance between sites available for bonding a^{T} at the edge of a zigzag tube $(n, 0)$, will depend on the tube parameter n as:

$$a^{\mathrm{T}} = \frac{\sqrt{3} a^{\mathrm{Gr}} n}{\pi} \sin\frac{\pi}{n}, \tag{1}$$

where $a^{\mathrm{Gr}} = 2.46$ Å is a distance between atomic sites at the zigzag edge of graphene. For example, according to formula (1) the inter-site distance a^{T} will be 2.35 Å for a $(6, 0)$ nanotube and 2.45 Å for a $(24, 0)$ nanotube, respectively. The distortions, introduced by tube curvature, can be adjusted so that a system decreases its energy. For example, the inter-site distances of the nanotubes relaxed with the bond-order potential [13] become 2.445 and 2.457 Å for the $(6, 0)$ and $(24, 0)$ tubes, respectively. The corresponding atomic energies of the relaxed nanotubes are 7.1 eV/atom and 7.37 eV/atom for the $(6, 0)$ and $(24, 0)$ tubes, respectively.

According to the pattern of sites available for bonding on the (111) diamond surface, it is possible to connect sites in the shape of a polygon with any number of segments N (starting with $N = 3$) of equal lengths $a^{\mathrm{D}} = 2.52$ Å. Depending on N, angles at vertices of a corresponding polygon can vary (Fig. 2). To obtain chemical bonding between a $(n, 0)$ nanotube and the corresponding N-sided polygon formed by dangling bonds on a diamond surface, the shape of the polygon should be as close as possible to circular to mimic that of a nanotube edge. Using formula (1), it is possible to evaluate the total mismatch between a nanotube of perimeter L_{T} and the perimeter of a polygon on the diamond surface L_{D}:

$$\delta_{\mathrm{tot}} = \frac{L_{\mathrm{D}} - L_{\mathrm{T}}}{L_{\mathrm{D}}} = \frac{a^{\mathrm{D}} - a^{\mathrm{T}}}{a^{\mathrm{D}}}, \tag{2}$$

For example, the total mismatch for a $(6, 0)$ nanotube is 6.7%, while that for $(24, 0)$ nanotube would be only 2.6%. Such strain, and even higher values as shown below, can be easily accommodated by the nanotube because of its high flexibility.

Second to total mismatch, which just reflects the changing of the inter-site distance at a tube edge as the tube curvature is changed, the most important feature determining stability is local mismatch. The local mismatch can be defined as the distance between a vertex of a polygon on a diamond surface and the point of the projection of a corresponding atom from a nanotube edge (Fig. 2). As it can be seen from Fig. 2, some of the interface bonds are more locally deformed for nanotubes of bigger radius, so indicating higher local mismatch. For $(6, 0)$ and $(24, 0)$ nanotubes this local mismatch would be 0.17 and 0.68 Å, respectively. A particular local mismatch can be more easily accommodated if a nanotube diameter is large because strain can be redistributed among a larger number of bonds of neighboring atoms. In addition, as discussed above, nanotubes with bigger radii posses less total mismatch with a polygon formed by atomic sites on a diamond surface, so that the interface energy of the relaxed structures is less for nanotubes with larger radii (Table III). Side and top views of relaxed $(6, 0)$ and $(24, 0)$ nanotubes attached to a (111) diamond surface are illustrated in Fig. 5.

Six distinct groups of nanotubes with different geometrical rules of bond formation can be identified depending on a parameter n of an $(n, 0)$ nanotube (Fig. 2). For every group of nanotubes, atomic sites on a diamond surface that participate in bonding between a nanotube and diamond form a specific polygon (in particular a hexagon). The shape of these hexagons, which should be close to circular, is defined by the constraint that a particular polygon should be obtained from a particular number of the segments of length a^{D} with fixed ends. The geometrical details of the hexagons are summarized in Table II. Energetic and structural characteristics of nanotubes of different groups are summarized in Table III.

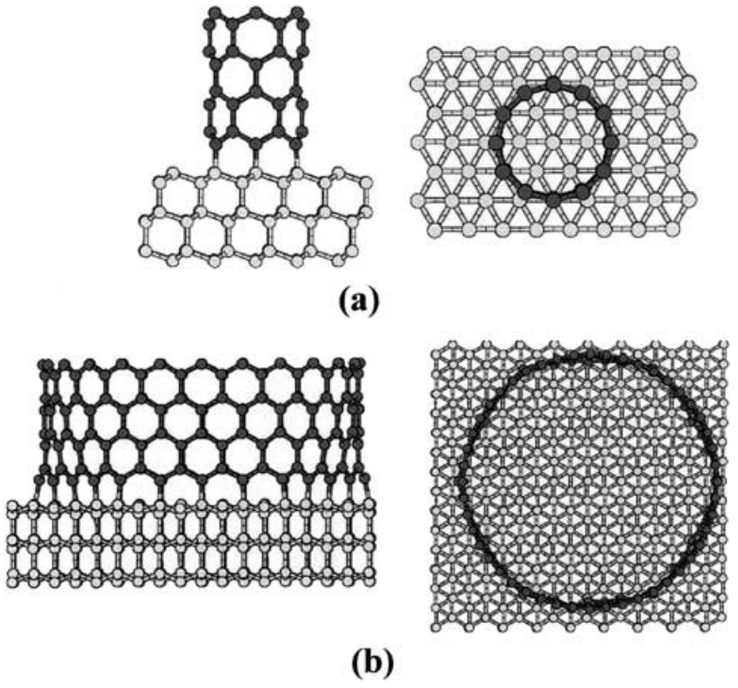

FIGURE 5 Relaxed hybrid structures of (a) $(6,0)$ and (b) $(24,0)$ nanotubes attached to a (111) diamond surface.

The first distinct group of nanotubes corresponds to nanotubes with a six-fold symmetry, namely $(6\times M,0)$ nanotubes, where M is an integer (Fig. 2a). Nanotubes of this group posses relatively low mismatches and low interface energies (Table III). The second group of nanotubes with a favorable geometry for bond formation is $(6\times M+3,0)$ nanotubes. The corresponding polygon on a diamond surface possesses three-fold symmetry (Fig. 2b). This group of nanotubes also possesses a relatively low degree of local mismatch with the diamond surface (Fig. 2b) and consequently has a low interface energy (Table III).

The next two groups of nanotubes are denoted by $(6\times M+2,0)$ and $(6\times M+4,0)$. The corresponding polygons on the diamond surface posses two-fold symmetry (Figs. 2c and d). Because the shape of the diamond polygons is elongated along one of their diameters, the tube shape near the interface becomes elliptic. Of these two groups of nanotubes, more favorable bonding with the (111) diamond surface occurs for the $(6\times M+4,0)$ group. Also, nanotubes from these two groups are semiconductiong, while those from the two previous are metallic. Therefore relatively strong chemical bonding with a (111) diamond surface for nanotubes with different electronic structures is feasible.

The two final groups of nanotubes, the geometry for which can be described as $(6\times M+1,0)$ and $(6\times M-1,0)$, will have dangling bonds (Fig. 2e and f)). The shape of the corresponding polygons is irregular and significantly deviates from circular along one of their sides. Not being completely flexible, nanotubes cannot accommodate such distortions. Characteristics of bonding for a $(7,0)$ nanotube are provided in Table III.

For zigzag nanotubes attached to a (111) diamond surface, it was demonstrated that if geometrical conditions are favorable, the total mismatch can be as low as 2.4% and strong chemical bonds between the components can be formed. A relatively wide variety

TABLE II Characteristic nanotube groups and parameters of the corresponding polygons on diamond surfaces formed by atomic sites available for bonding

Type of nanotubes	*Polygon sides (number & lengths)*	*Comments*
$(6\times M,0)$, $M=1,2,3\ldots$	$6\times Ma^{D}$	
$(6M+2,0)$	$2\times(M+1)a^{D}$; $4\times Ma^{D}$	
$(6M+3,0)$	$3\times(M+1)a^{D}$; $3\times Ma^{D}$	
$(6M+4,0)$	$4\times(M+1)a^{D}$; $2\times Ma^{D}$	
$(6M+1,0)$	$3\times Ma^{D}$; $2\times(M+1)a^{D}$; $1\times(M-1)a^{D}$	M dangling bonds along the same side
$(6M+5,0)$	$3\times Ma^{D}$; $2\times(M-1)a^{D}$; $1\times(M+1)a^{D}$	M dangling bonds along the same side

TABLE III Energetic characteristics and bond lengths for various nanotube/diamond interfaces

		Average energy per atom (eV)		
Nanotube type	*Interface energy (J/m²)*	*Diamond*	*Nanotube*	*Interface bond lengths (Å)*
Zigzag nanotubes and the (111) diamond facet				
(6, 0)	0.53	−7.45	−6.84 (−7.1)	1.525
(12, 0)	0.74	−7.44	−7.0 (−7.32)	1.525 (6), 1.529 (6)
(18, 0)	0.75	−7.43	−7.04 (−7.36)	1.52 (12), 1.537 (6)
(24, 0)	0.78	−7.42	−7.05 (−7.37)	1.52 (12), 1.547 (6), 1.519 (6)
(8, 0)	1.04	−7.38	−6.85 (−7.22)	1.51 (3), 1.53 (4), 1.69 (1)
(9, 0)	0.58	−7.48	−6.95 (−7.26)	1.52 (6), 1.53 (3)
(10, 0)	0.61	−7.45	−6.99 (−7.28)	1.53 (6), 1.55 (4)
(7, 0)	15 (d.b.)	−7.43, −5.5 (d.b.)	−6.92 (−7.17), −4.57 (d.b.)	1.51 (4), 1.57 (2), 1d.b.
Armchair nanotube and a pentaparticle				
(5, 5)*	5 (0.9)	−6.85 (−7.0)	−6.2 (−7.45)	1.6 (1.6)
Zigzag nanotube and the (100) diamond facet				
(6, 0)	1.7	−7.4	−6.7	0.52 (2), 1.57 (2), 1.63 (2)
(8, 0)	1.2	−7.47	−6.83	1.47 (2), 1.54 (4), 1.62 (2)
(12, 0)†	1.6	−7.0	−7.0	1.48 (2), 1.52 (4), 1.57 (4)

Values in parentheses for bond lengths correspond to the number of bonds of the given length at the interface. In the column "nanotube", the value in parentheses corresponds to the energy per atom for a relaxed single nanotube (reference point for the interface energy calculations). Radical sites are denote by d.b. (dangling bond). *Values in parenthesis correspond to a structure with hydrogen atoms attached to the (5, 5) nanotube atoms near the interface to decrease the energy. †A (12, 0) nanotube attached to the dimerized diamond surface (Fig. 7).

of types of nanotubes are available for bonding due to the low mismatch between sites available for bonding at the (111) surface and those at a zigzag tube edge. Another important factor is a high density of surface sites on the (111) diamond surface that posses six-fold symmetry and thus every surface atom has six neighbors in a plane. This provides more flexibility for curving a line of attachment of a sheet of graphene to the surface. This line can be deviated from a straight line by 30 or 90 degrees without changing the distance between sites available for bonding. As shown below, for the (100) diamond surface the situation is less favorable. Due to the four-fold symmetry of the surface sites at a (100) surface, deviation of a line of attachment from a straight line without changing the distance between sites available for bonding is possible through curving by 90 degrees only. Another possible deviation by 45 degrees is accompanied by changing the inter-site distance by a factor of $\sqrt{2}$. While this strain can still be accommodated by a nanotube as demonstrated by results of atomistic simulations below, the interface energy is noticeably higher than other structures.

Bonding of Armchair Nanotubes with a Diamond Pentaparticle

In the previous section hybrid structures of zigzag nanotubes attached to the (111) diamond surface were discussed. Because armchair nanotubes have sites alternating from 1.42 to 2.84 Å along the edge, patterns of sites available for bonding at the (111) diamond surface is not favorable for bond formation. However, there exists a particular diamond cluster, called a pentaparticle, which has a surface pattern consisting of five (111) surfaces separated by twin grain boundaries and an axis of symmetry oriented along the ⟨110⟩ direction (Fig. 6). Diamond pentaparticles have been observed experimentally as free standing structures resulting from vapor phase growth [15] as well as five-fold microcrystals embedded in chemical vapor deposited diamond films. Sites available for bonding at the intersection of twin boundaries with a surface are only about 1.55 Å away from each other. The distance between other sites available for bonding on (111) diamond surfaces is about 2.54 Å. Thus a pattern of sites available for bonding on a surface of a pentaparticle mimics that at an edge of the armchair (5, 5) nanotube. The total mismatch is about −4.1%. Energetic characteristics of the interface are summarized in Table III. A relaxed hybrid structure constructed from a (5, 5) nanotube and a pentaparticle is illustrated in Fig. 7.

Another class of armchair nanotubes with five-fold symmetry, $(5 \times M, 5 \times M)$ nanotubes, can also be attached to a penta-particle with all bonds saturated at the interface. However, the total mismatch increases with increasing nanotube radius because some of the 1.42 Å inter-site distances at a nanotube edge will correspond to 2.54 Å distances between the diamond sites. However, the simulations predict that the local mismatch can be accommodated at least for nanotubes with $M = 2, 3$ (Fig. 6).

Bonding of Zigzag Nanotubes with (100) Diamond

Because of the four-fold symmetry of the (100) diamond surface, the polygons that contour the surface sites with the shape closest to circular are octagons and squares (Fig. 8). While in general an octagon more closely resembles a circular shape than a hexagon, four of the segments in the surface

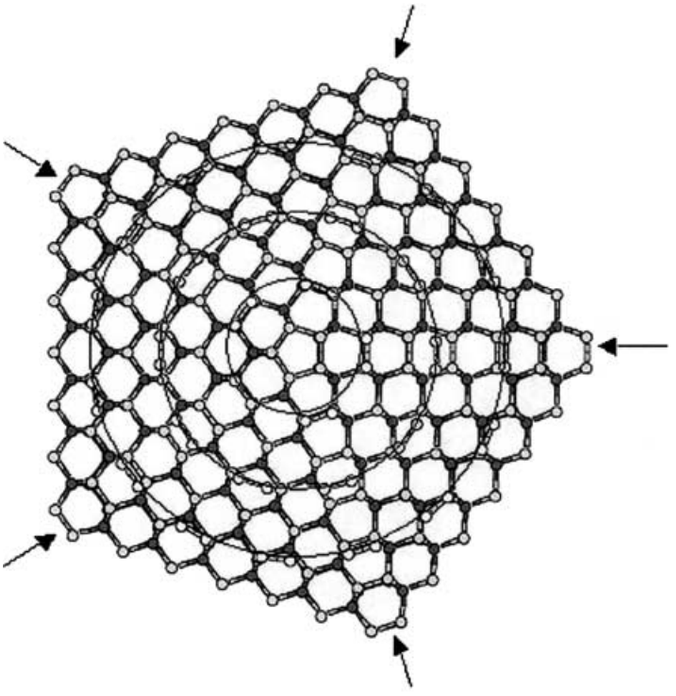

FIGURE 6 Scheme of the possible connection between a diamond pentaparticle along the ⟨110⟩ axis and the armchair $(5n, 5n)$, $n = 1–3$ nanotubes. Solid lines indicate the contours of attachment of the corresponding nanotubes. Light circles along the solid lines correspond to the sites available for bonding at the nanotube edges. Grey circles correspond to the sites available for bonding on the nanoparticle surface. The (111) surfaces, those are seen at the projection, are inclined to the plain of the projection (see also Fig. 5). Arrows indicate the twin grain boundaries.

octagons have an inter-site distance $\sqrt{2}a^{\mathrm{D}}$. This value is 45% larger than that in a nanotube and therefore hinders bonding with a nanotube. After analyzing numerous possibilities for bonding (100) surfaces (both unreconstructed and reconstructed) with different types of zigzag nanotubes, it was concluded that it is not possible to develop general schemes for tube attachment as in a case of the (111) surface and zigzag nanotubes ("Bonding between Nanotubes and (111) Diamond Facet" Section). Most hybrid structures contained dangling bonds at the interface. In some cases, however, it was possible to construct structures with all bonds saturated at the interface

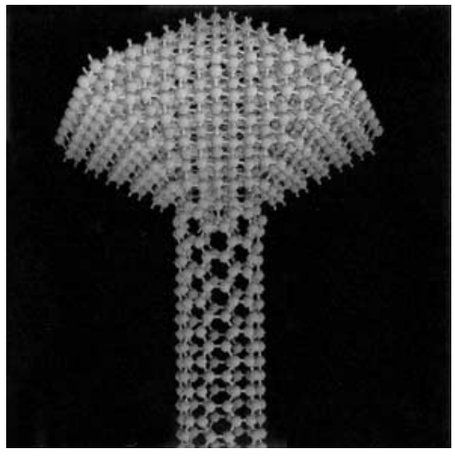

FIGURE 7 Illustration of the relaxed hybrid interface structure between a diamond pentaparticle and a $(5, 5)$ nanotube.

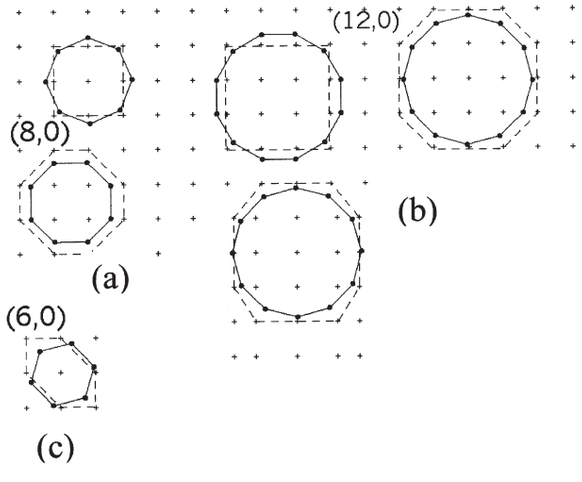

FIGURE 8 Schemes of the possible connection between the (100) diamond surface and zigzag nanotubes. Dots connected by solid lines correspond to atomic sites available for bonding at nanotube edges. Crosses correspond to atomic sites at the (100) diamond surface. Dashed lines connect sites on the diamond surface participating in the bonding with the specific nanotube.

for both metallic and semiconducting types of nanotubes; those are illustrated below.

Figure 8a illustrates a possible connection between a (100) diamond surface and (8, 0) nanotube. The total mismatch with the surface sites contouring the square is only 4.9%, and the simulations predict that the local mismatch 0.49 Å can be easily accommodated by the nanotube. Another possible bonding with an interface contour in a shape of an octagon is illustrated in Fig. 8a. For this type of connection, the total mismatch is 22% and the local mismatch 0.83 Å, which is much bigger than in the previous type. Atoms at the unreconstructed (100) surface are twofold coordinated and after connecting with a nanotube. they remain unsaturated. The dangling bonds at the interface can trap electrons and suppress conductivity through the interface. Therefore for electronic applications of these types of structures, models of hybrid structures with all bonds saturated should be considered. It can be either surface reconstruction (e.g. dimer formation) or hydrogen passivation. For the above hybrid structure of the (8, 0) nanotube with the diamond surface sites contouring a square, hydrogen atoms were also attached to the interface atoms from the diamond side. The interface characteristics of the relaxed structure are provided in Table III.

Possible types of connection of the (12, 0) nanotube with the diamond surface are illustrated in Fig. 8b. Total mismatches are 3.4%, 15% and 9% for the square, octagon and an octagon on the reconstructed diamond surface, respectively. The maximum local mismatch is ~ 0.7 Å for the square and ~ 1 Å for the octagons on both the reconstructed and unreconstructed diamond surfaces. Atomistic simulation was performed for the hybrid structure of a (12, 0) nanotube connected with the reconstructed diamond surface where only addition of two hydrogen atoms was required to saturate all dangling bonds at the interface. The interface characteristics are summarized in Table III.

Atomistic simulation was also performed for a hybrid structure of another metallic nanotube, (6, 0), bonded to the (100) diamond surface with a contour of the interface corresponding to a hexagon (Fig. 8c). Despite the high total (18%) and maximal local (1.2 Å) mismatches, the nanotube was able to accommodate the introduced distortions, although the interface energy is high. The interface characteristics are summarized in Table III.

From the discussion above, there are a limited number of zigzag nanotubes that can be attached to a (100) diamond surface with all bonds at the interface saturated (by surface reconstruction or through adding hydrogen). In addition to the hybrid structures composed of (6, 0), (8, 0) and (12, 0) nanotubes on diamond (100) discussed above, (16, 0) and (18, 0) nanotubes on diamond (100) are also possible. Although the interface energies for these nanotubes and the (100) diamond surface are higher those for the nanotubes and the (111) diamond surface, they are still reasonable. For example, grain boundaries energies in diamond are about $2-4\,J/m^2$ [16] and the average energy per atom in a fullerene is about -6.84 eV. These energy values are comparable or even higher then the interface energies of diamond/nanotube hybrid structures (Tables I and III) or energy per atom for atoms at the interface, respectively.

CONCLUSION

Based on geometrical considerations and detailed atomic modeling, it has been shown that particular combinations of nanotubes and diamond surfaces can form chemically and mechanically stable interfaces. The atomistic simulations also suggest that significant lattice mismatches between a diamond surface and a nanotube can be accommodated by nanotubes due to their high radial flexibility. Thus, in principle, chemically bonded hybrid structures between selected nanotubes and silicon carbide surfaces may also be stable.

These results support experimental evidence suggesting the formation of nanotube structures attached to diamond clusters formed during high temperature annealing, and expand upon and generalize prior modeling studies of these systems [10,11]. The analysis presented here also suggests that it may be possible to produce a wide array of structurally robust hybrid nanotube-diamond interfaces that could have applications in structural materials and nanoelectronic device components. An example of using discussed hybrids as functional nanostructures can be a proximal probe tip consisting of a nanotube strongly attached via chemical bonds to a diamond cantilever.

Acknowledgements

The financial support of the Office of Naval Research under contract N00014-95-1-0270, and through a Multi-University Research Initiative is gratefully acknowledged. Dr V. Zhirnov is thanked for helpful discussions.

References

[1] Kuznetsov, V.L., Chuvilina, A.L., Butenkoa, Y.V., Stankusb, S.V., Khairulinb, R.A. and Gutakovskiic, A.K. (1998) "Closed curved graphite-like structures formation on micron-size diamond", *Chem. Phys. Lett.* **289**, 353.

[2] Kuznetsov, V.L., Zilberberg, I.L., Butenko, Y.V., Chuvilin, A.L. and Segall, B. (1999) "Theoretical study of the formation of closed curved graphite-like structures during annealing of diamond surface", *J. Appl. Phys.* **86**, 863.

[3] Avigal, Y. and Kalish, R. (2001) Abstract Book, *12th European Conference on Diamond, Diamond-like materials, Carbon nanotubes, Nitrides & Silicon Carbides*, Budapesht, Hungary, September.
[4] Ayres, V., Wright, B., Asmussen, J., Song, S., *et al.* (2000) *Electrochem. Soc. Proc.* **12**, 236.
[5] Lambrecht, W., Lee, C.H., Segall, B., Angus, J.C., Li, Z. and Sunkara, M. (1993) "Diamond nucleation by hydrogenation of the edges of graphitic precursors", *Nature* **364**, 607.
[6] Shenderova, O. and Brenner, D.W. (1997) "Coexistence of two carbon phases at grain boundaries in polycrystalline diamond", *Mat. Res. Symp. Proc.* **442**, 693.
[7] Balaban, A.T., Klein, D.J. and Folden, C.A. (1994) "Diamond graphite hybrids", *Chem. Phys. Lett.* **217**, 266.
[8] Davidson, B.N. and Pickett, W.E. (1994) "Graphite-layer formation at a diamond (111) surface step", *Phys. Rev. B* **49**, 14770.
[9] de Vita, A., Galli, G., Canning, A. and Car, R. (1996) "A microscopic model for surface-induced diamond-to-graphite transitions", *Nature* **379**, 523.
[10] Sinnott, S.B., Shenderova, O.A., White, C.T. and Brenner, D.W. (1997) "Mechanical Properties of nanotubule fibers and composites determined from theoretical calculations and simulations", *Carbon* **36**, 1.
[11] Shenderova, O.A. and Brenner, D.W. (2002) "Simulation of grain boundaries, triple junctions and related disclinations". In: Klimanek, P., Romanov, A.E., Seefeldt, B.M., (eds), *Local Lattice Rotations and Disclinations in Microstructures of Distorted Crystalline Materials, Solid State Phenom.*, Trans. Tech. Publ., Switzerland, **Vol. 87**, p. 318.
[12] Shenderova, O.A., Areshkin, D. and Brenner, D.W. *Mater. Res.*, Submitted for publication.
[13] Brenner, Donald W., Shenderova, Olga A., Harrison, Judith A., Stuart, Steven J., Ni, Boris and Sinnott, Susan B. (2002) "Second Generation Reactive Empirical Bond Order (REBO) potential energy expression for hydrocarbons", *J. Phys.: Condens. Matter* **14**, 783–802.
[14] Li, Z., Wang, L., Suzuki, T., Argoitia, A., Pirouz, P. and Angus, J. (1993) "Orientation relationship between chemical vapor-deposited diamond and graphite substrates", *J. Appl. Phys.* **73**, 711.
[15] Matsumoto, S. and Matsui, Y. (1983) "Electron-microscopic observation of diamond particles grown from the vapor-phase", *J. Mat. Sci.* **18**, 1785.
[16] Shenderova, O.A., Brenner, D.W., Nazarov, A.A., Romanov, A.E. and Yang, L.H. (1998) "Multiscale modeling approach for calculating grain boundaries energies from first principles", *Phys. Rev. B* **57**, R3181.